

Isogeometric Simulation and Shape Optimization with Applications to Electrical Machines



Peter Gangl, Ulrich Langer, Angelos Mantzaflaris,
and Rainer Schneckleitner

Abstract Future e-mobility calls for efficient electrical machines. For different areas of operation, these machines have to satisfy certain desired properties that often depend on their design. Here we investigate the use of multipatch Isogeometric Analysis (IgA) for the simulation and shape optimization of the electrical machines. In order to get fast simulation and optimization results, we use non-overlapping domain decomposition (DD) methods to solve the large systems of algebraic equations arising from the IgA discretization of underlying partial differential equations. The DD is naturally related to the multipatch representation of the computational domain, and provides the framework for the parallelization of the DD solvers.

1 Introduction

Isogeometric Analysis (IgA) is a relatively new approach for discretizing partial differential equations (PDEs). IgA was introduced in [2]. It can be seen as an alternative to the more classical Finite Element Method (FEM). The idea in IgA

P. Gangl

Institute of Applied Mathematics, TU Graz, Graz, Austria

e-mail: gangl@math.tugraz.at

U. Langer

Institute of Computational Mathematics, JKU Linz, Linz, Austria

RICAM, Austrian Academy of Sciences, Linz, Austria

e-mail: ulanger@numa.uni-linz.ac.at

A. Mantzaflaris

Institute of Applied Geometry, JKU Linz, Linz, Austria

Université Côte d'Azur, Inria Sophia Antipolis - Méditerranée, Valbonne, France

e-mail: angelos.mantzaflaris@jku.at

R. Schneckleitner (✉)

RICAM, Austrian Academy of Sciences, Linz, Austria

e-mail: rainer.schneckleitner@ricam.oeaw.ac.at

© Springer Nature Switzerland AG 2020

G. Nicosia, V. Romano (eds.), *Scientific Computing in Electrical Engineering, Mathematics in Industry* 32, https://doi.org/10.1007/978-3-030-44101-2_4

is to use the same basis functions for both representing the geometry of the computational domain and solving the PDEs. This aspect makes IgA especially interesting for design optimization procedures. In practice, it is often the case that one performs design optimization and geometric modeling simultaneously. State-of-the-art computer aided design (CAD) software uses B-splines or Non-Uniform Rational B-splines (NURBS) for the modeling process whereas the design optimization requires an analysis suitable representation of the model. So far the design optimization is mainly done using FEM as discretization method. Hence, the B-spline or NURBS representation of the geometric model has to be converted into a suitable mesh for the Finite Element Analysis. This conversion is in general very computationally demanding. The new IgA paradigm circumvents these problems. Therefore, IgA is very beneficial for the simulation and optimization when the representation of the computational domain comes from CAD software; see [1, 10] for applications to electrical machines.

Since practical optimization problems tend to be very large, the numerical solution of the underlying PDEs becomes computationally very expensive. Moreover, in PDE-constrained shape optimization processes, there are more than one PDE to solve. In particular, line search requires to solve the magnetostatic PDE constraint several times. In order to get fast optimization results, we use Dual-Primal Isogeometric Tearing and Interconnecting (IETI-DP) methods for the solution of the linear algebraic systems arising from the IgA discretization. The IETI-DP solvers are non-overlapping domain decomposition methods; see [5, 6]. IETI-DP methods are closely related to the FEM-based FETI-DP methods; see, e.g., [9] and the references therein. We show that IETI-DP methods are superior to sparse direct solvers with respect to computational time and memory requirement. Moreover, IETI-DP provides a natural framework for parallelization. Indeed, our numerical experiments on a distributed memory computer show an excellent scaling behavior of this method.

The remainder of the paper is organized as follows. In Sect. 2, we describe our model problem and the shape optimization method that is based on the shape derivative. Section 3 is devoted to the IETI-DP solver and its performance on parallel computers. Finally, in Sect. 4, we use IETI-DP within the interior point optimizer Ipopt [11] yielding an efficient shape optimization procedure.

2 Shape Optimization via Gradient Descent

2.1 Problem Description

We investigate the simulation and shape optimization of an interior permanent magnet (IPM) electric motor by means of IgA. The IgA approach seems to be very attractive for such practical problems. The most beneficial aspect of IgA in the context of optimization is the fact that the same basis functions which are used

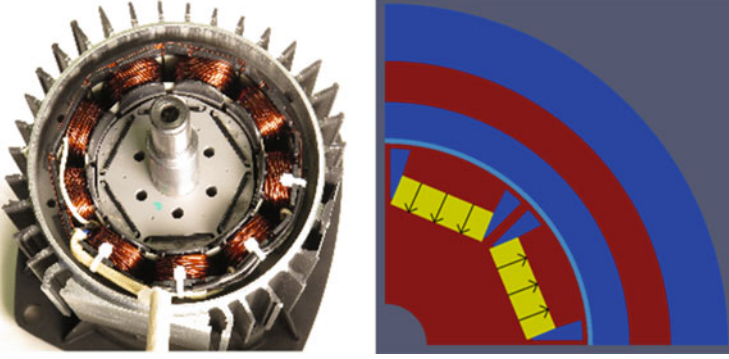


Fig. 1 Real world IPM electric motor (see Acknowledgement section) on the left, and a quarter of the cross section of a similar electric motor with 8 magnetic poles that is used in our numerical tests on the right

to represent the geometry of the IPM electric motor are also exploited to solve the underlying PDEs. In the optimization procedure, we want to optimize the shape of the motor in order to maximize the runout performance, i.e. to maximize the smoothness of the rotation of the motor. An example of an IPM electric motor is given in Fig. 1 (left). One possible way to optimize the runout performance of an IPM electric motor is to minimize the squared L^2 -distance between the radial component of the magnetic flux B in the air gap and a desired smooth reference function B_d . The resulting optimization problem is subject to the 2d magnetostatic PDE as constraint.

Mathematically, the arising optimization problem can be expressed as follows:

$$\min_D J(u) := \int_{\Gamma} |B(u) \cdot \mathbf{n}_{\Gamma} - B_d|^2 ds = \int_{\Gamma} |\nabla u \cdot \boldsymbol{\tau}_{\Gamma} - B_d|^2 ds \quad (1)$$

$$\text{s.t. } u \in H_0^1(\Omega) : \int_{\Omega} \nu_D(x) \nabla u \cdot \nabla \eta \, dx = \langle F, \eta \rangle \quad \forall \eta \in H_0^1(\Omega), \quad (2)$$

where J denotes the objective function, Γ is the midline of the air gap, Ω denotes the whole computational domain, and D is the domain of interest also called design domain. The variational problem (2) is nothing but the 2d linear magnetostatic problem with the piecewise constant magnetic reluctivity $\nu_D(x) = \chi_{\Omega_f(D)}(x)\nu_1 + \chi_{\Omega_{\text{mag}}}(x)\nu_{\text{mag}} + \chi_{\Omega_{\text{air}}(D)}(x)\nu_0$. Here, Ω_f , Ω_{mag} and Ω_{air} denote the ferromagnetic, permanent magnet and air subdomains, respectively, and ν_1 , ν_{mag} and ν_0 denote the corresponding reluctivity values. Note that the shape D enters the optimization problem via the function ν_D and influences the objective function via the solution u . The right hand side $F \in H^{-1}(\Omega)$ in (2) is defined by the linear functional

$$\langle F, \eta \rangle := \int_{\Omega} (J_3 \eta + \nu_{\text{mag}} M^{\perp} \cdot \nabla \eta) \, dx \quad (3)$$

for all $\eta \in H_0^1(\Omega)$. Here, M^\perp denotes the perpendicular of the magnetization M , which is indicated in Fig. 1 and vanishes outside the permanent magnets, and J_3 is the third component of the impressed current density in the coils. Note that the solution u is the third component of the magnetic vector potential, i.e. $B(u) = \text{curl}((0, 0, u)^T)$. Moreover, $n_\Gamma = (n_1, n_2, 0)^T$ and $\tau_\Gamma = (\tau_1, \tau_2)^T$ denote the outward unit normal and unit tangential vectors along the air gap, respectively.

We are interested in the radial component of the magnetic flux density along the air gap due to the permanent magnetization. For that reason, we set $J_3 = 0$ and consider the coil regions as air. Figure 1 (right) shows a quarter of a cross section of a simplified IPM electric motor that is provided by CAD software. Hence, this geometry representation is suitable for IgA simulation. The red-brown areas represent ferromagnetic material (Ω_f), the blue areas consist of air (Ω_{air}), the yellow areas are the permanent magnets (Ω_{mag}). The air gap of the motor is highlighted in light blue. In this initial model for the optimization, the design domain D is the ferromagnetic area right above the permanent magnets. In order to get a smoother rotation we are looking for a better shape of this part D .

2.2 The Shape Derivative

For the optimization of the IPM electric motor, we use gradient based optimization techniques. Hence, we need the derivative of the objective J with respect to a change of the current shape. The shape derivative in tensor form [4, 7, 10] of our optimization problem is given by

$$dJ(D)(\phi) = \int_{\Omega} \mathcal{S}(D, u, p) : \partial\phi dx, \quad \forall \phi \in H_0^1(\Omega, \mathbb{R}^2) \quad (4)$$

with $\mathcal{S}(D, u, p) = (v_D(x)\nabla u \cdot \nabla p - v_{\text{mag}}\nabla p \cdot M^\perp)\mathcal{J} + v_{\text{mag}}\nabla p \otimes M^\perp - v_D(x)\nabla p \otimes \nabla u - v_D(x)\nabla u \otimes \nabla p$, where \mathcal{J} denotes the identity, the state u solves the constraint (2), and p solves the adjoint problem

$$\int_{\Omega} v_D(x)\nabla p \cdot \nabla \eta dx = -2 \int_{\Gamma} (B(u) \cdot n_\Gamma - B_d)(B(\eta) \cdot n_\Gamma) ds \quad \forall \eta \in H_0^1(\Omega). \quad (5)$$

In (4), $\mathcal{S}(D, u, p) : \partial\phi$ means Frobenius' scalar product of the 2×2 matrices $\mathcal{S}(D, u, p)$ and $\partial\phi = (\frac{\partial\phi_i}{\partial x_j})_{i,j=1}^2$, defined by $A : B := \sum_{i=1}^n \sum_{j=1}^n a_{ij}b_{ij}$ for general $n \times n$ matrices $A = (a_{ij})_{i,j=1}^n$ and $B = (b_{ij})_{i,j=1}^n$, whereas $a \otimes b := (a_i b_j)_{i,j=1}^n$ for vectors $a = (a_i)_{i=1}^n$ and $b = (b_j)_{j=1}^n$ from \mathbb{R}^n .

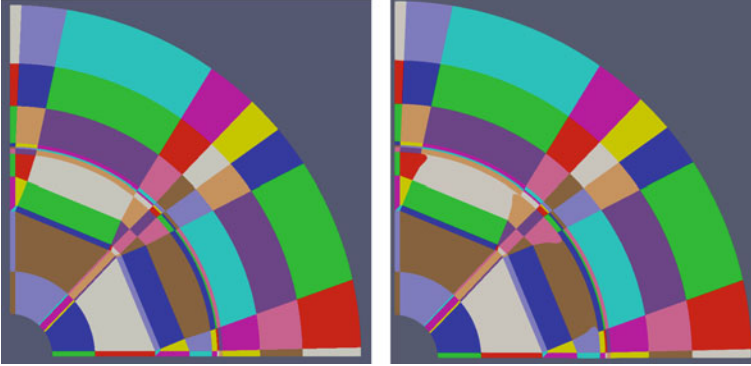


Fig. 2 Initial and final design of an IPM motor

2.3 Numerical Shape Optimization

We used a continuous Galerkin (cG) IgA discretization for both the simulation and optimization problems. The implementation is done in **G+Smo**.¹ Figure 2 (left) shows a possible computational domain suitable for cG. The shown multipatch domain consists of 93 patches. For each of these patches, we used a B-spline mapping from a reference patch with splines of degree 3. For the optimization, we need the shape gradient $\nabla J \in V := H_0^1(\Omega, \mathbb{R}^2)$ which can be computed by solving the auxiliary problem: find $\nabla J \in V$ such that

$$b(\nabla J, \psi) = -dJ(D)(\psi) \quad \forall \psi \in V. \quad (6)$$

The expression on the right hand side of (6) is the negative shape derivative whereas the expression $b(\cdot, \cdot)$ on the left hand side is some V -elliptic, V -bounded bilinear form which must be chosen appropriately. For our studies, we used

$$b(\phi, \psi) = \int_{\Omega} \phi \cdot \psi \, dx + \int_{\Omega} \alpha(\partial\phi : \partial\psi) \, dx \quad (7)$$

with a patchwise constant function $\alpha \in L^\infty(\Omega)$.

In the right picture of Fig. 2, we can see the optimized shape with respect to the runout performance compared to the initial domain on the left. We were able to reduce the objective from $4.236 \cdot 10^{-4}$ down to $2.781 \cdot 10^{-4}$.

¹Mantzaflaris, A. et al.: G+Smo (geometry plus simulation modules) v0.8.1., <http://gs.jku.at/gismo>, 2017 Jun 19 2018.

3 Fast Numerical Solutions by IETI-DP

Up to now, we have solved the arising PDEs by means of a sparse direct solver. One drawback of a direct solution method is that it is rather slow for large-scale systems. In particular, in shape optimization, we have to solve the state equation (2), the adjoint equation (5), and the auxiliary problem (6) for the shape gradient, which decouples into two scalar problems, in every iteration of the optimization algorithm. Moreover, during a line search procedure, it might be the case that the state equation has to be solved several times. To overcome the issue of a slow performance, we were looking for a fast and suitable solver for our simulation and optimization processes. We chose the IETI-DP technique for solving the PDEs [5]. IETI-DP is a non-overlapping domain decomposition technique which introduces local subspaces which are then again coupled using additional constraints. A comparison between the sparse direct solver SuperLU [3] and IETI-DP for solving the state equation (2) on a full cross section of an IPM electric motor clearly shows that the recently developed IETI-DP method [5] performs much better as can be seen in Table 1. The numerical results displayed in Tables 1 and 2 were obtained on RADON1 (<https://www.ricam.oeaw.ac.at/hpc/overview/>) a high performance computing cluster with 1168 computing cores and 10.7 TB of memory. Table 1 also shows that, with an increasing number of degrees of freedom, the proposed IETI-DP technique solves the problem much faster than the sparse direct solver. Moreover, it can be seen that, with too many degrees of freedom, the sparse direct solver ran out of memory whereas IETI-DP could provide the solution to the problem. The solution to the state equation is shown in Fig. 3 (right).

Moreover, IETI-DP provides a natural framework for parallelization. Because of the multipatch structure of the computational domains in IgA, each patch can be seen as a subdomain in the IETI-DP approach. Then one can create suitable subdomains consisting of a certain number of patches for each processor, e.g., one possible choice is to group the patches to subdomains according to their number of degrees of freedom which means that the degrees of freedom are almost evenly distributed over the number of processors. Table 2 shows the strong scaling behavior of the IETI-DP solver. In this experiment, we solved the constraint equation (2) on

Table 1 SuperLU vs. IETI-DP on a single core

# dofs	SuperLU	IETI-DP	speedup
72,572	36.0 s	17.0 s	2.12
250,844	193.0 s	69.8 s	2.77
928,796	1943.0 s	463.0 s	4.20
3,570,332	–	1179.0 s	–

Table 2 Strong scaling with IETI-DP and 3,570,332 dofs

# cores	1	2	4	8	16	32	64	128
Time [s]	1179	577	325	164	89	43	22	14
Rate	–	2.04	1.78	1.98	1.84	2.07	1.95	1.57

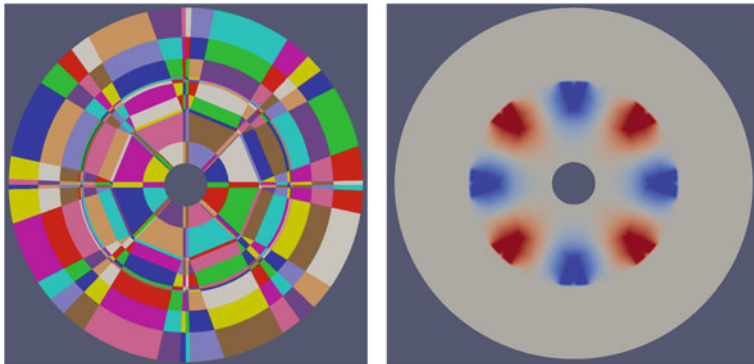


Fig. 3 Whole initial cross section as well as the solution

the full cross section of an IPM electric motor with 3,570,332 degrees of freedom. From Table 2, we can see the expected performance, i.e., if we double the number of processors the computation time reduces nearly by a factor of two.

4 Shape Optimization Based on Ipopt and IETI-DP

In this section, we point out the usage of the interior point optimizer Ipopt [11], for the shape optimization using IETI-DP as underlying PDE solver. If we perform shape optimization without any additional considerations, then we might run into troubles. More precisely, it can happen that we get self-intersections in the final shape even if the objective decreases.

To prevent such self-intersections, we consider the Jacobian determinant of the geometry transformation in the design domain and its neighboring air regions. The Jacobian determinant of these patches must have the same sign in each iteration. If the sign changes from one iteration to the next, then we reduce the step size until the Jacobian determinant of the new design has the same sign as in the initial configuration. In this way, we are able to ensure that the shape is technically feasible.

In the first naive approach, all control coefficients of the multipatch domain are considered as design variables, and the vector field computed by (6) is applied globally. The computational effort for the optimization can be reduced by applying the computed vector field only on the important interfaces between the design domain and the neighboring air regions. This reduces the number of design variables from approximately 28,000 to 128 in the coarsest setting. The inner control coefficients of the design area and the bordering air regions are rearranged via a spring patch model [8].

In a first test setting, Ipopt stops at an optimal solution after 95 iterations using a BFGS method. We set the NLP error tolerance to 10^{-6} , the relative error in the objective change to the same value, and we decided to exit the optimization loop

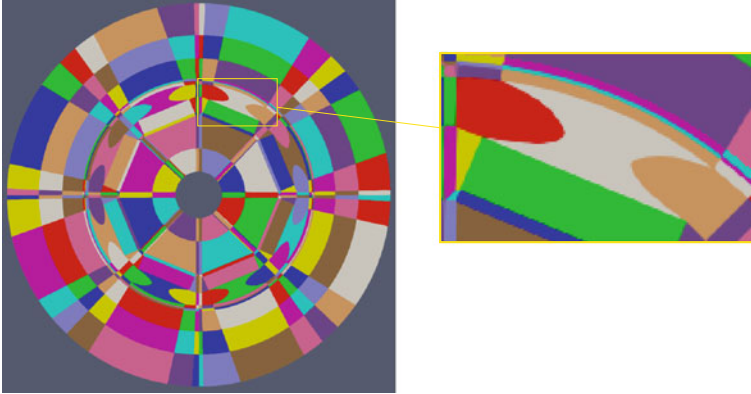


Fig. 4 Optimal shape after 130 iterations with relaxed bounds (left), zoom into one of the design regions (right)

after three iterations within these error bounds. The objective value dropped from $4.266 \cdot 10^{-4}$ down to $2.587 \cdot 10^{-4}$

Furthermore, we tried an additional experiment where we relaxed the bounds on the constraints a bit. In particular, we set the `bound_relax_factor` in `Ipopt` to 1. The result of this experiment can be seen in Fig. 4. We may observe from Fig. 4 that we get a very smooth final shape with even a smaller objective value of $2.436 \cdot 10^{-4}$. We point out that, if we adjust the different optimization parameters, we may get different optimal shapes and different objective values in the end.

Acknowledgments This work was supported by the Austrian Science Fund (FWF) via the grants NFN S117-03 and the DK W1214-04. We also acknowledge the permission to use the Photo in Fig. 1 (left) taken by the Linz Center of Mechatronics (LCM). The motor was produced by Hanning Elektro-Werke GmbH & Co KG.

References

1. Bontinck, Z., Corno, J., Schöps, S., De Gerssem, H.: Isogeometric analysis and harmonic stator-rotor coupling for simulating electric machines. *Comput. Methods Appl. Mech. Eng.* **334**, 40–55 (2018)
2. Cottrell, J.A., Hughes, T.J.R., Bazilevs, Y.: *Isogeometric analysis: CAD, finite elements, NURBS, exact geometry and mesh refinement*. *Comput. Methods Appl. Mech. Eng.* **194**, 4135–4195 (2005)
3. Demmel, J.W., Eisenstat, S. C., Gilbert, J.R., Li, X.S., Liu, J. W. H.: A supernodal approach to sparse partial pivoting. *SIAM J. Matrix Anal. Appl.* **20**(3), 720–755 (1999)
4. Gangl, P.: *Sensitivity-based topology and shape optimization with application to electrical machines*. Ph.D. thesis, Johannes Kepler University Linz (2016)
5. Hofer, C., Langer, U.: Dual-primal isogeometric tearing and interconnecting solvers for multipatch dG-IgA equations. *Comput. Methods Appl. Mech. Eng.* **316**, 2–21 (2017)

6. Kleiss, S., Pechstein, C., Jüttler B., Tomar S.L.: IETI–isogeometric tearing and interconnecting. *Comput. Methods Appl. Mech. Eng.* **247**, 201–215 (2012)
7. Laurain, A., Sturm, K.: Distributed shape derivative via averaged adjoint method and applications. *Esaim Math. Model. Numer. Anal.* **50**(4), 1241–1267 (2016)
8. Nguyen, D.M., Gravesen, J., Evgrafov, A.: Isogeometric analysis and shape optimization in electromagnetism. Ph.D. thesis, Technical University of Denmark (2012)
9. Pechstein, C.: Finite and Boundary Element Tearing and Interconnecting Solvers for Multiscale Problems. Springer, Berlin (2013)
10. Schneckenleitner, R.: Isogeometrical analysis based shape optimization. Master thesis, Johannes Kepler University Linz (2017)
11. Wächter, A., Biegler, L.T.: On the implementation of an interior-point filter line search algorithm for large scale nonlinear programming. *Math. Program.* **106**(1), 25–57 (2006)